

**THIOL-ENE PHOTO CROSSLINKING POLYMERIZATION AS AN
ALTERNATIVE APPROACH TO DEVELOPING HYDROXIDE EXCHANGE
MEMBRANES**

by

Stephen Robert Masinde Ekatan

A thesis submitted to the Faculty of the University of Delaware in partial fulfillment of the requirements for the degree of Master of Materials Science and Engineering

Fall 2012

© 2012 Stephen Robert Masinde Ekatan
All Rights Reserved

**THIOL-ENE PHOTO CROSSLINKING POLYMERIZATION AS AN
ALTERNATIVE APPROACH TO DEVELOPING HYDROXIDE EXCHANGE
MEMBRANES**

by

Stephen Robert Masinde Ekatan

Approved: _____
Christopher Kloxin, Ph.D.
Professor in charge of thesis on behalf of the Advisory Committee

Approved: _____
David C. Martin, Ph.D.
Chair of the Department of Materials Science and Engineering

Approved: _____
Babatunde Ogunnaike, Ph.D.
Dean of the College of Engineering

Approved: _____
Charles G. Riordan, Ph.D.
Vice Provost for Graduate and Professional Education

ACKNOWLEDGMENTS

I consider it an honor to have worked with Professor Christopher Kloxin and thank him immensely for the opportunity to join his research group, his flexibility, continuous advice, guidance, and academic support.

I would like to thank my committee members, Professor Xinqiao Jia, Professor Yushan Yan and Professor John Rabolt for their expert feedback and contribution to my research.

I am indebted to Professor Shuang Gu for his guidance and support in the area of fuel cell membranes and ion conductivity testing, to Tom Cristiani, Kloxin Research Group, who has made available his support in so many ways and to Ngoc Nguyen, Mackay Research Group, for his support in the area of membrane mechanical testing.

This manuscript is dedicated to;

The Ekatan family for their unconditional love. I could not have achieved this goal without their unending love, patience and understanding.

TABLE OF CONTENTS

LIST OF TABLES	vi
LIST OF FIGURES	vii
ABSTRACT	viii

Chapter

1	INTRODUCTION	1
2	EXPERIMENTAL	6
2.1	Materials	6
2.2	Synthesis and Membrane Fabrication Methodology	6
2.2.1	Synthesis of BPAAE, Compound A in Figure 5	10
2.2.2	Synthesis of CMBPAAE, Compound B in Figure 5	11
2.2.3	Synthesis of QBPAAE-Cl, Compound C in Figure 5	12
2.2.4	Membrane Fabrication and Hydroxide Exchange(Alkalization)	13
2.3	Water Uptake and Swelling Ratio (Dimensional Stability)	16
2.4	Hydroxide Conductivity (HC)	17
2.5	Ion Exchange Capacity (IEC)	18
2.6	Tensile Strength	19
3	RESULTS AND DISCUSSION	20
3.1	Chemical Stability	20
3.2	Hydroxide Conductivity and IEC	20
3.3	Water Uptake and Swelling Ratio (Dimensional Stability)	22
3.4	Mechanical Properties	23

3.5	Strategy for Increased Hydroxide Conductivity	26
4	CONCLUSION	28
5	PATH FOWARD	30
	REFERENCES	31
	Appendix	
	<i>RAW DATA FOR WATER UPTAKE AND SWELLING RATIO</i>	33

LIST OF TABLES

Table 1: Molecular Weights of Monomers in Ternary System	14
Table 2: Composition of Ternary Mixture before Photo Crosslinking	14
Table 3: Raw Data for Hydroxide Conductivity (HC) and IEC	20
Table 4: Summary of Water Uptake Swelling Ratio	22
Table 5: Mechanical Properties of Membranes	23
Table A6:Raw Data for Water Uptake and Swelling Ratio Experiments	33

LIST OF FIGURES

Figure 1: Chemical structure of Nafion [®]	1
Figure 2: Working Principles of a hydrogen-based HEMFC	2
Figure 3: Chemical equations of a HEMFC	3
Figure 4: Ternary monomer system	7
Figure 5: Synthesis of QBPBAE-Cl	8
Figure 6: Structure of PETMP	10
Figure 7: NMR spectra for BPAE	11
Figure 8: NMR spectra for CMBPAE	12
Figure 9: NMR spectra for QBPBAECl	13
Figure 10: Stress vs. Strain Graphs for Membrane 1: 15	24
Figure 11: Stress vs. Strain Graphs for Membrane 1:2	24
Figure 12: Synthesis of QDMPBPAE	27

ABSTRACT

An alternative and new approach to making hydroxide exchange membranes (HEM's) for hydroxide exchange membrane fuel cells (HEMFC) via thiol-ene photo-crosslinking polymerization is demonstrated. Specifically a novel difunctional vinyl monomer, quaternary phosphonium bisphenyl allyl ether chloride (QPBPAAE-Cl), was successfully synthesized in a simple and cost effective three-step process. This synthesis protocol enables the interchangeability of the cationic functional group in the last synthesis step to readily assess hydroxide conductivity differences. This novel charged monomer was successfully photo-crosslinked in a ternary system consisting of 1,6-hexanedithiol and 1,3,5-Triallyl-1,3,5-triazine-2,4,6(1H,3H,5H)-trione (TATATO, a trifunctional 'ene' for crosslinking) to form the HEM. While the formed HEMs exhibit low hydroxide conductivity, they possess robust mechanical properties and excellent alkaline stability in 1M KOH for 48 hrs. The hydroxide conductivity for 200 – 290 μm thick specimens was 1.4 and 2.6 mScm^{-1} for a QPBPAAE-Cl to TATATO ratio of 1:1.5 and 1:2, respectively, and a stoichiometric balance of thiol monomer. The swelling ratio of the HEM was 8.25% and 8.89% in water and the measured tensile strength was 57.73 and 45.28 MPa for a QPBPAAE-Cl to TATATO ratio of 1:1.5 and 1:2, respectively.

Chapter 1

INTRODUCTION

Fuel cells have evolved into a promising and interesting alternative source of electric power in the recent years. This electric power is generated from chemical energy when a fuel, such as hydrogen or methanol, is consumed. In general, a fuel cell consists of anode and cathode layers separated by either an ion conducting electrolyte or membrane. The membrane is the key component in a fuel cell because of its role as an ion carrier (ionic conductor) and a barrier for gas and electrons (electronic insulator). The most widely used fuel cell is the proton exchange membrane fuel cell (PEMFC) that uses Nafion[®], (see Figure 1) a DuPont perfluorosulfonic acid polymer, as the ion conductive polymer. ^{1, 2, 3, 4}

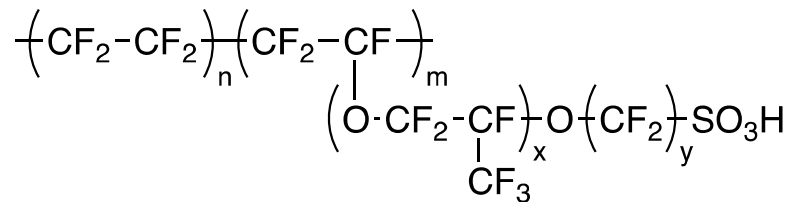


Figure 1: Chemical structure of Nafion[®]

Holistically Nafion[®] possesses all the ideal properties under operating conditions of PEMFC (below 100°C), which include high ionic conductivity, good chemical resistance and dimensional stability; however, the drawbacks to Nafion[®] are high fuel crossover, high cost of operation ($\sim \$160\text{kW}^{-1}$), environmental issues with manufacturing, and the need for expensive precious metals as catalysts in the anode and cathode.^{1, 2, 3, 4}

Recent research has focused on another type of fuel cell, the hydroxide exchange membrane fuel cell (HEMFC, see Figure 2 and Figure 3), as a potential replacement of the PEMFC.

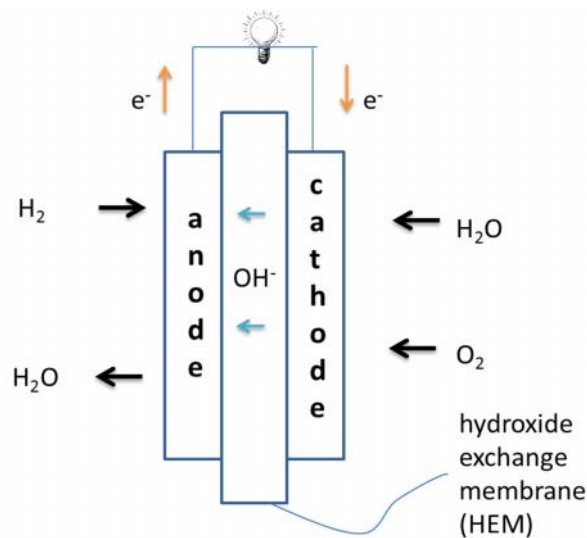


Figure 2: Working principles of a hydrogen-based HEMFC

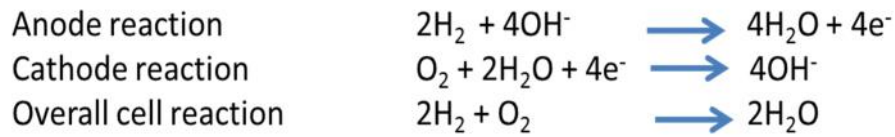


Figure 3: Chemical equations of a HEMFC

In a PEMFC, conditions are acidic and protons are transferred from the anode to the cathode through a proton exchange membrane. Conversely, in a HEMFC conditions are alkaline and hydroxide ions are transferred from the cathode through a hydroxide exchange membrane (HEM) to the anode. The alkaline conditions in a HEMFC enhance the chemical reactions at the electrodes and the flow of hydroxide ions opposes fuel crossover. Therefore HEMFC has several advantages over PEMFCs, such as rapid electrochemical kinetics on non-precious metal catalysts for a range of fuels and low fuel crossover.⁵ To be a viable option, HEMs must meet performance, durability and cost targets. To meet performance and durability targets, HEMs need good mechanical, thermal and chemical stability in alkaline conditions, high ion conductivity ($>100 \times 10^{-3} \text{ S cm}^{-1}$), selectivity to prevent fuel and electron crossover yet allow for free passage of ions. The charge on the membrane and degree of crosslinking affect the mechanical properties of HEMs. A higher degree of crosslinking improves mechanical strength while higher charge on the membrane reduces the mechanical strength because it promotes swelling of the membrane. The nature of the cationic group and polymer backbone determine the chemical stability of the membrane. The cationic group and polymer backbone need to be stable in alkaline conditions, the

operating conditions of HEMs. An attack on the cationic group results in the reduction of anionic exchange groups and therefore a decrease in the ion conductivity while an attack on the polymer backbone results in the degradation of the membrane. The cationic group used in the HEMs influences the ion conductivity because it determines the concentration of charge and ionic mobility. Within the phosphonium cationic group, tris(2,4,6-trimethoxyphenyl)phosphine > tris(2,6-dimethoxyphenyl)phosphine > triphenylphosphine. To meet cost targets, the material and production costs should allow for profitability.^{2, 1}

Current routes of fabricating HEM materials typically add quaternary ammonium or quaternary phosphonium functional groups to commercially available high performance engineering polymers (e.g., polysulfone) via a very highly reactive nucleophilic substitution reaction between halogenomethyl (e.g., chloromethyl) group and a tertiary amine or phosphine molecule.⁵ The chloromethylation of these polymers often requires extended reaction times (multiple days) and harsh and expensive chemicals (e.g., stannous chloride).⁶

In this research I propose using thiol-ene photo crosslinking polymerization as an alternative approach to fabricating HEMs. Thiol-ene photopolymerization is a reaction involving the addition of a thiol function group to an alkene functional group via a radical-mediated step-growth addition mechanism. The advantages of thiol-ene photopolymerization are 1) spatial and temporal control over the progress of the reaction, 2) a step-growth reaction mechanism that produces a homogeneous polymer

network, 3) the polymerization is not inhibited by oxygen, and 4) the availability of an array of thiol and ene monomers enabling simple modification of membrane properties.^{7, 8, 9, 10, 11}

The focus on the research presented herein will be on 1) the synthesis of a new ionomer QBPAAE-Cl, 2) photocrosslinking a ternary system of 1,6 hexanedithiol, QBPAAECl and TATATO to create membranes, and 3) characterizing the mechanical strength, dimensional stability (water uptake, swelling ration), hydroxide conductivity and ion exchange capacity (IEC) of these membranes.

Chapter 2

EXPERIMENTAL

2.1 Materials

Bisphenol A (BPA), paraformaldehyde and 1,6-hexanedithiol were purchased from Sigma Aldrich. Allyl bromide and triphenylphosphine were purchased from Tokyo Chemical Industry (TCI). TATATO was purchased from Acros Organics. Potassium carbonate anhydrous, magnesium sulphate anhydrous, sodium carbonate, acetone, dichloromethane, diethyl ether, 37% aqueous HCl and acetic acid were all purchased from Fisher Scientific. IRGACURE 651 (I-651) was kindly donated from BASF (formally Ciba Specialty Chemicals). Plain microscope slides, precleaned (25 x 75 x 1.0 mm) from Fisher Scientific. Color coded shim 5" x 20" (UPC No. 44155, Color: Pink, thickness: 0.381 mm) from Precision Brand.

2.2 Synthesis and Membrane Fabrication Methodology

The photopolymerization of a mixture of multifunctional thiols and enes is a simple, robust, and efficient method for rapid production of membranes with excellent control over physical and mechanical properties. The monomers utilized

in this research are 1,6-hexanedithiol, 1,3,5-Triallyl-1,3,5-triazine-2,4,6(1H,3H,5H)-trione (TATATO, a triene crosslinker), and quaternary phosphonium bisphenyl allyl ether chloride (QPBPAAE-Cl), a new diene cationic monomer synthesized during this research (Figure 4). The QPBPAAE-Cl monomer is synthesized following a three-step procedure: 1) formation of the diallyl ether of Bisphenol A, 2) chloromethylation of the diallyl ether, and 3) addition of triphenylphosphine to form the cationic monomer (see Figure 5).

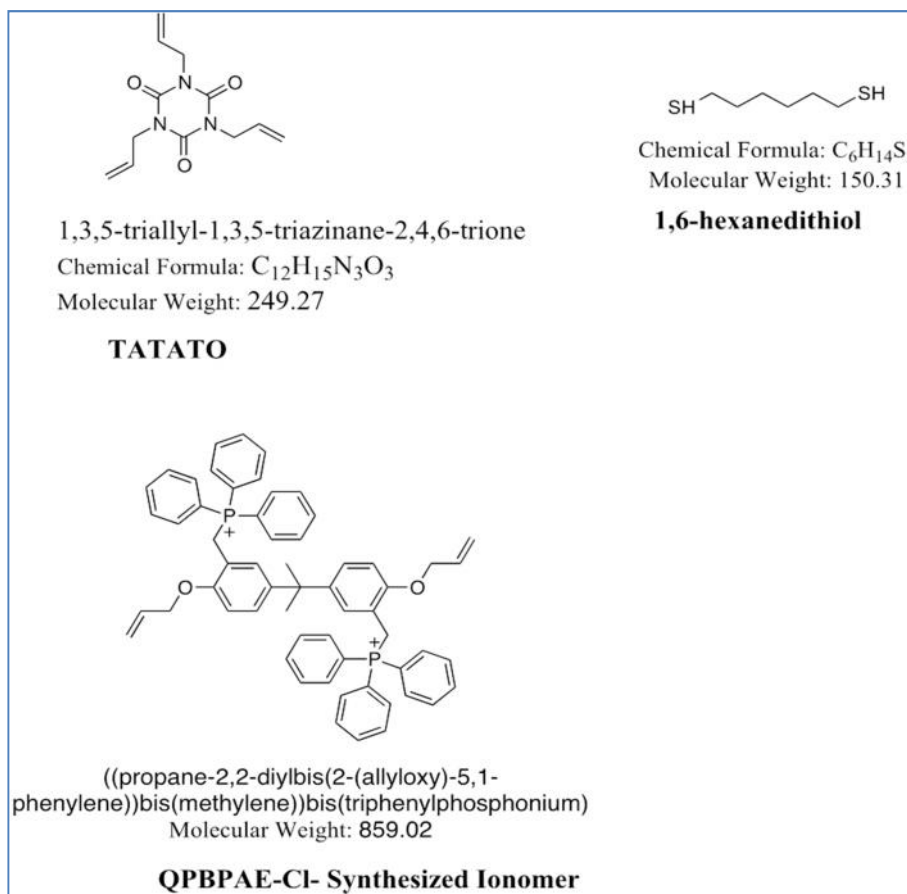


Figure 4: Ternary monomer system

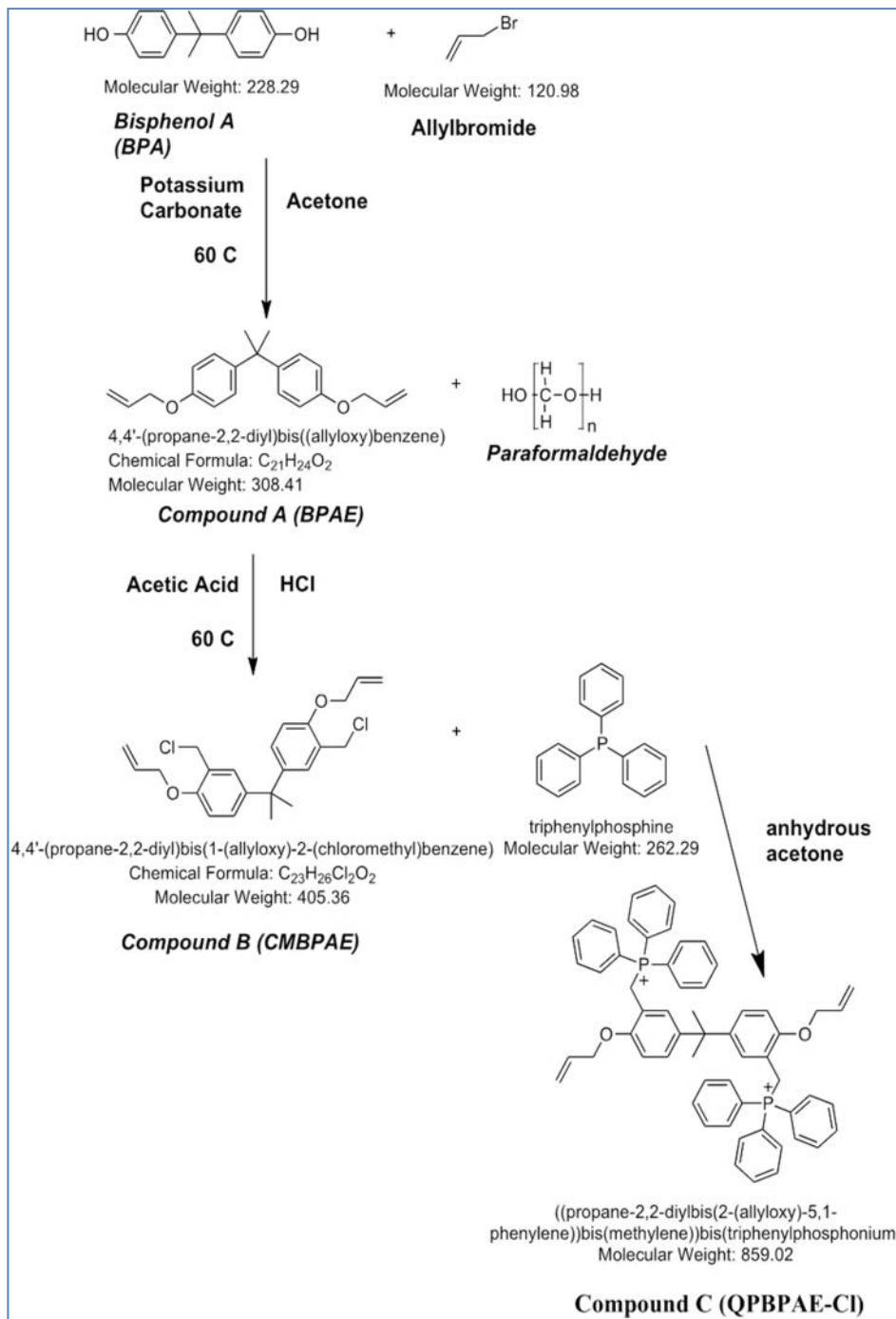


Figure 5: Synthesis of QBPBAE-Cl

The synthesis simplicity and the low cost of the monomers, makes this a particularly attractive approach to HEM fabrication. In contrast to linear polymers, chemically crosslinked polymer networks are, as a matter of definition, insoluble in all solvents. Moreover, the degree of swelling is readily controlled by the amount of crosslinker (i.e., TATATO) incorporated into the monomer mixture. The monomers are readily photopolymerized at room temperature using 3% wt IRGACURE 651(2,2-Dimethoxy-1,2-diphenylethan-1-one), a UV active photoinitiator widely used in thiol-ene reactions.¹²

The original proof-of-concept experiments utilized a binary monomer system containing a multifunctional thiol and ene, specifically Pentaerythritol tetra(3-mercaptopropionate) (PETMP) and QBPAAE-Cl. In this work, we demonstrated that QBPAAE-Cl is readily incorporated into a thiol-ene polymerization. Additionally, we showed that this radical-mediated reaction is not inhibited by the presence of a platinum catalyst, which is important when considering this material for application in the cathode and anode layers of the fuel cell. Unfortunately, it was discovered that the membranes formed with this material were not stable in alkaline medium, most likely owing to base-catalyzed ester degradation of the PETMP backbone (see PETMP structure in Figure 6). Based on this observation, a non-ester containing thiol monomer was selected for the studies presented herein.

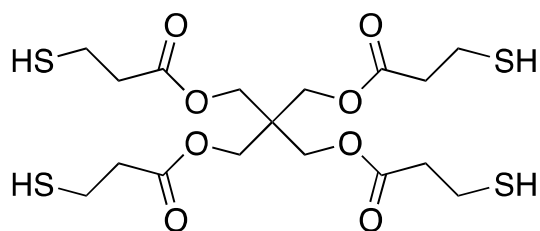


Figure 6: Structure of PETMP

2.2.1 Synthesis of BPAE, Compound A in Figure 5

The synthesis procedure by Nair et al. was used in the synthesis of BPAE. Specifically, BPA (11.2 g, 0.05 mol) was reacted with allyl bromide (13.06 g, 0.11 mol) in the presence of potassium carbonate (20.34 g, 0.15 mol) in approximately 200 ml of acetone at 60°C for 20 hrs. The residue was dissolved in 300 ml of dichloromethane and washed three times with 300 ml of 1 M dilute sodium carbonate solution. After drying over anhydrous magnesium sulphate (Mg_2SO_4), the residue was concentrated at reduced pressure until a colorless oil was obtained. It was characterized by proton NMR confirming the structure.¹³ The yield of this synthesis was 66%.

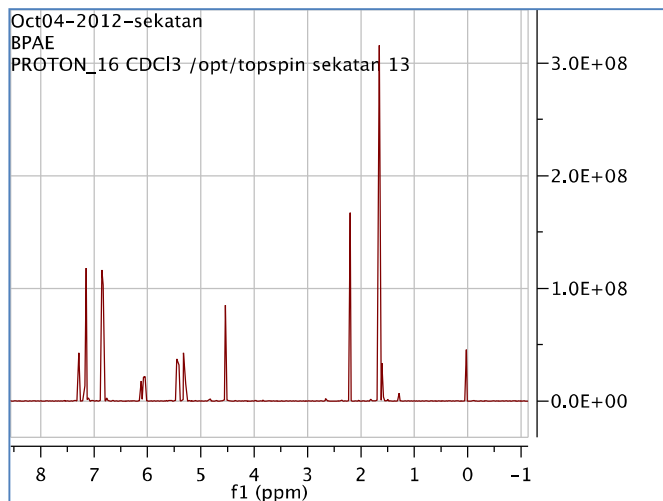


Figure 7: NMR spectra for BPAE

2.2.2 Synthesis of CMBPAE, Compound B in Figure 5

The synthesis procedure by Jaballah et al. was followed when synthesizing CMBPAE. Specifically, BPAE (9.376 g, 0.03 mol), paraformaldehyde (7.296 g, 0.24 mol of CH_2O), and 37% aqueous HCl (25.92 ml, 0.31 mol) in 250 ml of acetic acid was stirred at 60°C for 5 hrs. A combination of TLC and NMR was used to determine the unknown synthesis time. The resultant mixture was poured in 300 ml of dichloromethane and the organic layer washed three times with 300 ml of deionized water and dried over anhydrous Mg_2SO_4 and concentrated at reduced pressure until a yellow oil was obtained. It was characterized by proton NMR confirming the structure.¹⁴ The yield of this synthesis was 73%.

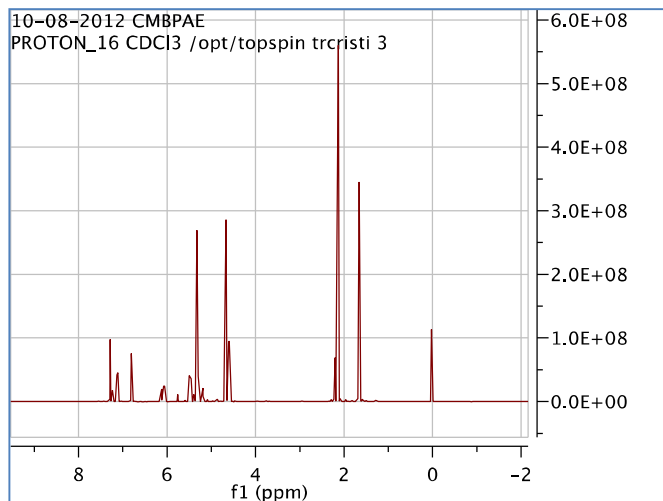


Figure 8: NMR spectra for CMBPAE

2.2.3 Synthesis of QPBPAE-Cl, Compound C in Figure 5

The procedure outlined by Jaballah et al. was followed for the synthesis of QPBPAECl. A solution of CMBPAE (8.918 g, 0.022 mol) and triphenylphosphine (12.694 g, 0.048 mol) in anhydrous acetone (150 mL) was stirred and heated at reflux for 13 hours in an argon atmosphere. A combination of TLC and NMR was used to determine the synthesis time. The reaction mixture was then cooled followed by stirring to initialize the precipitation. The white precipitate was filtered off and washed three times with 200 ml of diethyl ether and dried under vacuum overnight.¹⁴ The yield of this synthesis was 33%.

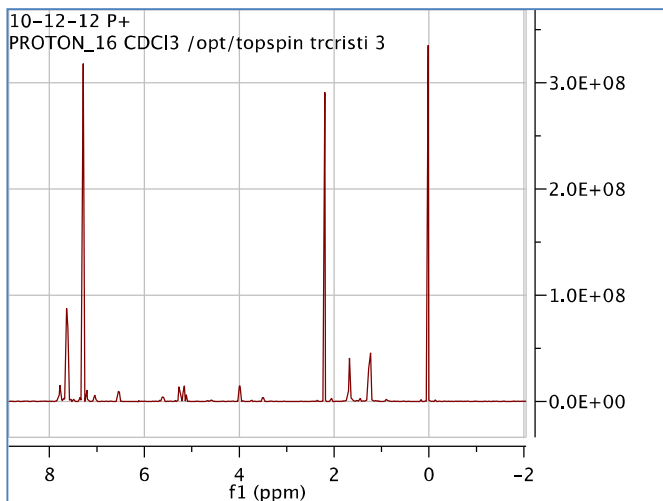


Figure 9: NMR spectra for QBPBAE-Cl

2.2.4 Membrane Fabrication and Hydroxide Exchange (Alkalization)

To fabricate the membrane, ternary systems of compositions in Table 1 were mixed. For each composition, 0.6 g of QBPBAE-Cl was used and dissolved using dichloromethane. The ternary mixture was transferred to a microscope slide prepared with a 0.381mm shim to provide an approximate thickness of 50 – 80 μm . The slides were then exposed to UV light with a 365nm filter for 480 s at an intensity of 50 W/cm^2 . The membranes were then placed in 1M KOH for 48 hours for exchange of Cl^- with OH^- (alkalization). The membranes were then carefully rinsed with deionized and placed in a tightly sealed container containing deionized water for at least 48 hours before any testing was done.

Table 1: Molecular Weights of Monomers in Ternary System

Monomer	MW (g/mol)	functional groups (FG)	MW/functional groups (g/mol)
QBPBAE-Cl	859.02	2	429.51
TATATO	249.27	3	83.09
1,6-hexanedithiol	150.31	2	75.155

Table 2: Composition of Ternary Mixture before Photo Crosslinking

Membrane	Mass QBPBAE-Cl (g)/(mol)	Mass TATATO (g)	Mass 1,6 hexanedithiol (g)/(mol)	Mass of 651 initiator (g)/(%)	Mole Ratio QBPBAE-Cl:TATATO
1	0.6027/1	0.1734/1.5	0.2591/2.5	0.0322/3	1:1.5
2	0.6009/1	0.2330/2	0.3233/3	0.0378/3	1:2

Example calculation of composition for membrane 1

$$Mass_{TATATO} = \frac{Mass_{QBPBAE-Cl}}{MW_{QBPBAE-Cl}} * \frac{Required\ Moles_{TATATO}}{Required\ Moles_{QBPBAE-Cl}} * \frac{MW_{TATATO}}{FG_{TATATO}} \dots \dots \dots \text{Equation 1}$$

$$Mass_{TATATO} = \frac{0.6027}{859.02} * \frac{1.5}{1} * \frac{249.27}{3} = 0.1748\ g$$

In Equation 1 above, $Mass_{TATATO}$ is the mass of TATATO required to achieve the targeted mole ratio, $Mass_{QPBAE-Cl}$ is the mass of QPBAE-Cl, $MW_{QPBAE-Cl}$ is the molecular weight of QPBAE-Cl, $FG_{QPBAE-Cl}$ is the number of functional groups in QPBAE-Cl, $\frac{Required Moles_{TATATO}}{Required Moles_{QPBAE-Cl}}$ is the mole ratio of TATATO: QPBAE-Cl, MW_{TATATO} is the molecular weight of TATATO and FG_{TATATO} is the number of functional groups in TATATO.

$$Mass_{dithiol} = \frac{Mass_{TATATO}}{MW_{TATATO}} * \frac{Required Moles_{dithiol}}{Required Moles_{TATATO}} * \frac{MW_{dithiol}}{FG_{dithiol}} \dots \dots \dots \text{Equation 2}$$

$$Mass_{dithiol} = \frac{0.1734}{\frac{249.27}{3}} * \frac{2.5}{1.5} * \frac{150.31}{2} = 0.2614 \text{ g}$$

In Equation 2, $Mass_{dithiol}$ is the required mass of 1,6-hexanedithiol, $\frac{Required Moles_{dithiol}}{Required Moles_{TATATO}}$ is the mole ratio of 1,6-hexanedithiol to TATATO, $MW_{dithiol}$ is the molecular weight of 1,6-hexanedithiol and $FG_{dithiol}$ is the number of functional groups in 1,6-hexanedithiol.

$$Mass_{651} = (Mass_{QPBAECl} + Mass_{TATATO} + Mass_{dithiol}) * \left(\frac{\%_{651}}{\%_{monomers}} \right) \dots \dots \dots \text{Equation 3}$$

$$Mass_{651} = 0.6027 + 0.1734 + 0.2591) * \left(\frac{3}{97} \right) = 0.0320 \text{ g}$$

In Equation 3, $Mass_{651}$ is the mass of I-651 initiator, $\%_{651}$ is the mass percent of I-651 indicator, and $\%_{monomers}$ is the percent weight of all the three monomers, QPBAE-Cl, TATATO and 1,6-hexanedithiol.

2.3 Water Uptake and Swelling Ratio (Dimensional Stability)

The method outlined by Yan et al. and summarized below was used to measure the water uptake and swelling ratio.⁵ Membranes were prepared and kept in a tightly sealed container containing deionized water for 10 hr to ensure full hydration. The weights and dimensions of the wet membranes were measured. The membranes were subsequently dried in an oven at 60⁰C for 48 h and weights and dimensions measured. The water uptake and swelling ratio were then calculated using equations 1 and 2 respectively.

$$\text{Water uptake (\%)} = \frac{W_{\text{wet}} - W_{\text{dry}}}{W_{\text{dry}}} \times 100 \dots \dots \dots \text{Equation 4}$$

In Equation 4 above, W_{wet} and W_{dry} are the weight of the wet and dry membranes respectively.

$$\text{Swelling ratio (\%)} = \frac{l_{\text{wet}} - l_{\text{dry}}}{l_{\text{dry}}} \times 100 \dots \dots \dots \text{Equation 5}$$

In Equation 5 above, l_{wet} and l_{dry} are average lengths of the wet and dry membranes respectively

$$\text{Where } l_{\text{wet}} = (l_{\text{wet}1} \times l_{\text{wet}2})^{\frac{1}{2}} \dots \dots \dots \text{Equation 6}$$

$$\text{And } l_{\text{dry}} = (l_{\text{dry}1} \times l_{\text{dry}2})^{\frac{1}{2}} \dots \dots \dots \text{Equation 7}$$

In Equations 6 and 7 above l_{wet1} , l_{wet2} and l_{dry1} and l_{dry2} are the lengths and widths of wet and dry membrane sample respectively.

2.4 Hydroxide Conductivity (HC)

The procedure outlined by Yan et al. and summarized below was followed.⁵ Hydroxide conductivity was measured in deionized water by a typical four-electrode AC impedance method utilizing an Ivium Technologies A08001 impedance analyzer and a scanning frequency range of 1 – 10⁵ Hz. Briefly, this impedance analyzer consists of two platinum foils that act as current carriers and two platinum wires that act as potential sensors. Sample preparation involves storing membranes in a tight sealed container containing deionized water for at least 24 hours before any measurements are made. Based on the impedance derived resistance, the hydroxide conductivity of the membrane, σ , was calculated through the following equation

$$\sigma = \frac{L}{WdR} \dots \dots \dots \text{Equation 8}$$

In Equation 8 above, L is the distance between the two potential electrodes (set up as 10000), d is the thickness (μm), W is the width (cm) of the membrane samples and R is the resistance of the membrane (Ω) derived from the right-side intersect of semi-circle on the complex impedance plane with the Re(Z) axis. The units of σ are mScm^{-1}

2.6 Tensile Strength

The tensile strength and % strain at failure were evaluated using TA Instruments RSA3. The standard test of Hencky strain model was used with a deformation per second speed of 0.001s^{-1} at 22°C . The membrane samples were dried in an oven at 60°C for 48 hours. Then these membrane samples with sizes of 2 cm x 0.5 cm and thickness of 0.27 mm were placed between the grips of the testing machine.

Chapter 3

RESULTS AND DISCUSSION

3.1 Chemical Stability

No discoloration, disintegration or damage visually observed on membranes exposed to 1M KOH for 48 hours. This confirms the stability of the polymer backbone. The stability of the cationic triphenylphosphonium group was not confirmed in this research. This would require the measurement of IEC values during the exposure to 1M KOH.

3.2 Hydroxide Conductivity and IEC

Table 3: Raw Data for Hydroxide Conductivity (HC) and IEC

Mole Ratio QBPAAE-Cl :TATATO	Resistance ()	Thickness (μm)	Width (cm)	HC (mS cm^{-1})	IEC _{theo} (mmol g^{-1})
1:1.5	27578, 27268 27159, 27335-Avg	200	0.70	2.6	0.998
1:2	29606, 30049 30667, 30107-Avg	290	0.80	1.4	0.907

The thicknesses of the membranes are larger than expected. The targeted thickness range was 50-80 μm using a 380 μm shim. The shim thickness was chosen to account for shrinkage of the membrane as a result of loss of dichloromethane used to dissolve the QBPAAE-Cl. This shim thickness was selected after membranes using a 1:1 ratio of QBPAAE-Cl: TATATO were made using different shims, and it was discovered that 380 μm shims resulted in membranes in the range of 50-80 μm . Surprisingly, an increase in the TATATO crosslinker resulted in thicker membranes. This is illustrated by the larger membrane thickness for QBPAAE-Cl: TATATO ratios of 1:2 than 1:1.5.

The method for calculating actual IEC (IEC_m) was not sensitive enough for the low IEC values depicted by the IEC_{theo} values. Therefore no actual values were obtained.

The observed hydroxide conductivity in the membranes presented here is lower than other phosphonium-based HEMs in the literature that utilize a pendant trimethoxytriphenylphosphonium cation (typically $>50 \text{ mS cm}^{-1}$).^{17,18} Polymer networks formulated with one mole ratios of 1:1.5 and 1:2 QBPAAE-Cl:TATATO, respectively, exhibited excellent mechanical integrity. In contrast, membranes formulated with reduced crosslinker concentrations (i.e., 1.5:1 or 2:1 QBPAAE-Cl: TATATO, respectively) were difficult to handle and were inadequate for HEM fuel cell applications. Therefore, one of the limitations of this ternary system is that the hydroxide conductivity cannot be increased by introducing more QBPAAE-Cl. We will address possible strategies for overcoming these limitations in section 3.5 below

3.3 Water Uptake and Swelling Ratio (Dimensional Stability)

Table 4: Summary of Water Uptake and Swelling Ratio

Mole ratio	Rep	Swelling ratio (%)	Water Uptake (%)
1:1.5	1	8.34	25.44
	2	8.15	23.68
1:2	1	8.95	20.70
	2	8.84	19.77

The membranes formulated with QBPAAE-Cl in the ternary monomer systems exhibits good dimensional stability and the water uptake decreases with increasing crosslinking as expected. A higher water uptake is realized in the more charged membrane (i.e., 1:1.5 versus 1:2, QBPAAE-Cl:TATATO, respectively) owing to the increase hydrophilicity of the charged membrane. Additionally, it is expected that the reduced crosslinking should enable more swelling. The data from the two HEM's (shown in Table 4) shows that for our ratios, the swelling ratio increased with increasing crosslinking. See Appendix A for raw data used to calculate the water uptake and swelling ratio. A similar unexpected trend is observed with mechanical properties in section 3.4 below.

3.4 Mechanical Properties

Table 5: Mechanical Properties of Membranes

Mole ratio	Tensile Strength (MPa) (%)	Strain at Failure (%)	Tensile modulus (MPa)	0.2% offset yield strength (MPa)
1:1.5	57 ±4	6.8±0.2	20±2	30±5
1:2	45±2	50±2	17.9±1.2	15±3

Although both samples show a high tensile strength, the trend deviates from the theory of rubber elasticity. An increase in crosslink density would typically result in a stiffer material with higher tensile strength, tensile modulus and lower strain at failure therefore we should expect the 1:2 HEM to have a higher tensile strength, tensile modulus and lower strain at failure than the 1:1.5 HEM. However our data shows a reversed trend with the 1:1.5 HEM having a higher tensile strength, tensile modulus and lower strain at failure. The 1:1.5 HEM (less crosslinked) shows a behavior of a brittle material (see Figure 10) while the 1:2 HEM (more crosslinked) shows a behavior of a ductile material (see Figure 11).

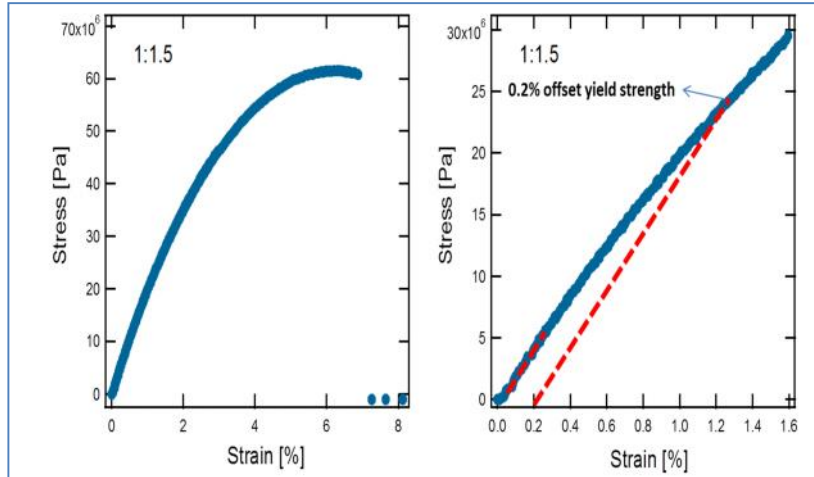


Figure 10: Stress vs. Strain Graphs for Membrane 1:1.5

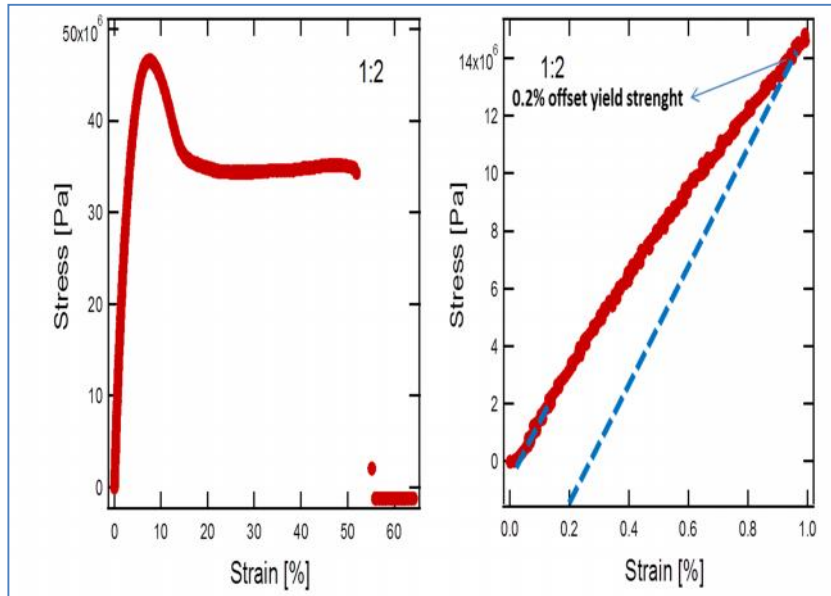


Figure 11: Stress vs. Strain Graphs for Membrane 1:2

The unusual trend in mechanical properties and swelling ratio observed above could be attributed to the stability of cationic group, the molecular weight per crosslink or the nature of charged polymers.

Tensile strength typically increases with increase in molecular weight. The 1:1.5 HEM has a higher molecular weight per crosslink than the 1:2 HEM as more high molecular weight charged monomer is incorporated and therefore it is possible that 1:1.5 HEM would have a higher tensile strength than the 1:2 HEM.

The stability of the phosphonium cation is enhanced by nature of its side groups. If the side groups are very large, then their steric bulk tends to protect the phosphorous atom from hydroxide. The presence of electron donating side groups and side groups participating in conjugation add stability by making the phosphorous atom electron rich. The side groups in triphenylphosphonium cation are phenyl groups which are electron withdrawing, do not participate in conjugation or provide adequate protection to the phosphorous atom from hydroxide attack. This makes the triphenylphosphonium cation very unstable. This instability could be an explanation to the unusual mechanical and swelling observations. In comparison, the 2,4,6-trimethoxyphenyl side groups in tris(2,4,6-trimethoxyphenyl)phosphonium cation are electron donating, participate in conjugation and due to their large size provide protection to the phosphorous atom from hydroxide attack. The triphenylphosphonium cation is known to be very stable.^{18, 19}

3.5 Strategy for Increased Hydroxide Conductivity

As mentioned above, the materials examined herein exhibited low hydroxide conductivity. One solution is to utilize a more basic phosphonium and in turn more hydroxide conducting cationic group like tris(2,6-dimethoxyphenyl)phosphine or tris(2,4,6-trimethoxyphenyl)phosphine. Another possible solution is to use a thiol crosslinker (i.e., a monomer with three or more thiol functional groups) that is stable in alkaline conditions. The use of this latter binary system would allow higher mole ratios of cationic monomer vs thiol without affecting the network formation. These two paths would create much higher hydroxide conductivities. As an illustration, a new cationic monomer was synthesized with tris(2,6-dimethoxyphenyl)phosphine as the cationic group (QDMPBPAE-Cl or Compound D in Fig 10) and photo crosslinked with 1,6-hexanedithiol and TATATO in a ratio of 1:1 for QDMPBPAE-Cl to TATATO. The formed membrane was stable in 1M KOH for 48 hours and had a hydroxide conductivity of 10.6 mScm^{-1} .

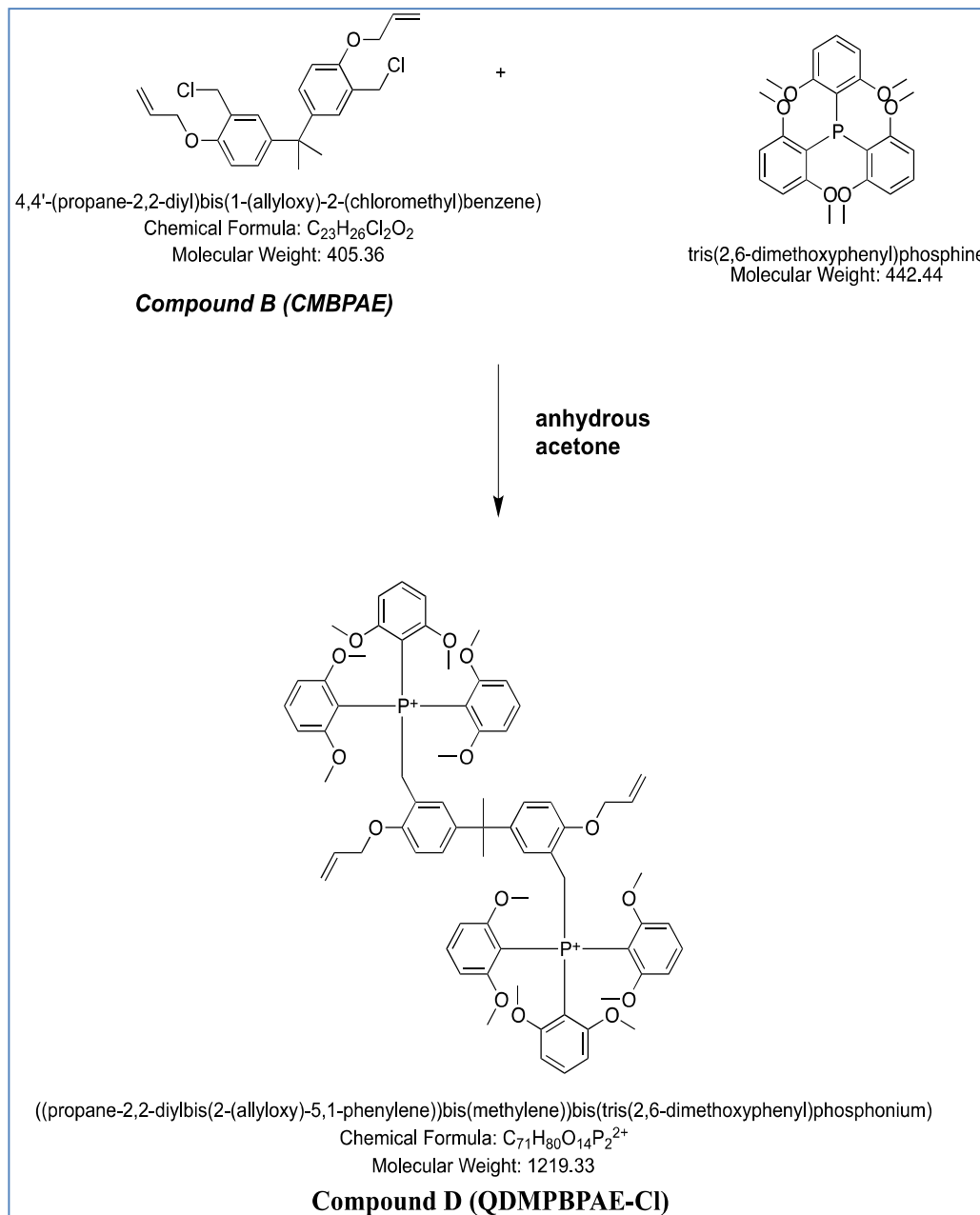


Figure 12: Synthesis of QDMPBPAE-Cl

Chapter 4

CONCLUSION

Thiol-ene photo-crosslinking has been demonstrated as a viable option to creating HEMs. The HEMs considered here have good chemical stability, dimensional stability and mechanical properties for applications in HEMFCs. A novel difunctional ene cationic monomer was synthesized in a simple and cost effect three-step process.

While the hydroxide conductivity fell short of the $>50 \text{ mScm}^{-1}$ target, we have identified promising avenues for conductivity improvements. Our HEMs have hydroxide conductivities of $1.4 - 2.6 \text{ mScm}^{-1}$, which is similar to other ammonium based crosslinked materials measured in the literature.²⁰ We have demonstrated that the use of tris(dimethoxyphenyl)phosphine would result in a hydroxide conductivity of 10 mScm^{-1} with a 1:1 mole ratio of QDMPBPAE -Cl:TATATO. Further hydroxide conductivity enhancements are possible with higher hydroxide conducting cationic groups such as tris(trimethoxyphenyl)phosphine. This would also address the unusual mechanical property and swelling ratio observations. Additionally, the switch to a binary system would allow for more cationic monomer to be added to the material

without significantly compromising the network forming ability of the HEM monomer system.

Chapter 5

PATH FOWARD

The next steps in this research include; 1) identify a new alkaline stable multifunctional thiol (>2), 2) use a binary system and vary the composition of thiol and ene to control the membrane morphology, 3) replace triphenylphosphine with tris(2,4,6-trimethoxyphenyl)phospine for higher ion conductivity and superior stability, 4) reduce the thickness of the HEMs by using thinner shims to hit the 50 - 80 μ m thickness target.

REFERENCES

1. Couture, G., Alaaeddine, A., Boschet, F. & Ameduri, B. Polymeric materials as anion-exchange membranes for alkaline fuel cells. *Progress in Polymer Science* **36**, 1521-1557 (2011).
2. Smitha, B., Sridhar, S. & Khan, A. A. Solid polymer electrolyte membranes for fuel cell applications—a review. *J. Membr. Sci.* **259**, 10-26 (2005).
3. Chen, S., Krishnan, L., Srinivasan, S., Benziger, J. & Bocarsly, A. B. Ion exchange resin/polystyrene sulfonate composite membranes for PEM fuel cells. *J. Membr. Sci.* **243**, 327-333 (2004).
4. Yamada, M. & Honma, I. Proton conducting acid–base mixed materials under water-free condition. *Electrochim. Acta* **48**, 2411-2415 (2003).
5. Yan, X. *et al.* Quaternized poly(ether ether ketone) hydroxide exchange membranes for fuel cells. *J. Membr. Sci.* **375**, 204-211 (2011).
6. Qiao, J., Fu, J., Liu, L., Liu, Y. & Sheng, J. Highly stable hydroxyl anion conducting membranes poly(vinyl alcohol)/poly(acrylamide-co-diallyldimethylammonium chloride) (PVA/PAADDA) for alkaline fuel cells: Effect of cross-linking. *Int J Hydrogen Energy* **37**, 4580-4589 (2012).
7. Klemm, E. & Beil, U. Unusual addition by the thiol-ene photopolymerization. *Polymer Bulletin* **28**, 653-656 (1992).
8. Such, G. K., Johnston, A. P. R., Liang, K. & Caruso, F. Synthesis and functionalization of nanoengineered materials using click chemistry. *Progress in Polymer Science* **37**, 985-1003 (2012).
9. Claudino, M., Johansson, M. & Jonsson, M. Thiol–ene coupling of 1,2-disubstituted alkene monomers: The kinetic effect of cis/trans-isomer structures. *European Polymer Journal* **46**, 2321-2332 (2010).
10. - Hoyle, C. & - Bowman, C. - Thiol–Ene Click Chemistry. - *Angewandte Chemie International Edition*, - 1540.
11. - Hoyle, C. E., - Lee, T. Y. & - Roper, T. - Thiol–enes: Chemistry of the past with promise for the future. - *Journal of Polymer Science Part A: Polymer Chemistry*, - 5301.
12. Nair, D. P., Cramer, N. B., Scott, T. F., Bowman, C. N. & Shandas, R. Photopolymerized thiol-ene systems as shape memory polymers. *Polymer* **51**, 4383-4389 (2010).
13. Reghunadhan Nair, C. P., Krishnan, K. & Ninan, K. N. Differential scanning calorimetric study on the Claisen rearrangement and thermal polymerisation of diallyl ether of bisphenols. *Thermochimica Acta* **359**, 61-67 (2000).

14. Jaballah, N. *et al.* Blue-luminescent poly(p-phenylenevinylene) derivatives: Synthesis and effect of side-group size on the optical properties. *European Polymer Journal* **47**, 78-87 (2011).
15. Xu, S. *et al.* Synthesis and properties of a novel side-chain-type hydroxide exchange membrane for direct methanol fuel cells (DMFCs). *J. Power Sources* **209**, 228-235 (2012).
16. Yan, X. *et al.* Imidazolium-functionalized polysulfone hydroxide exchange membranes for potential applications in alkaline membrane direct alcohol fuel cells. *Int J Hydrogen Energy* **37**, 5216-5224 (2012).
17. Gu, S. *et al.* Quaternary Phosphonium-Based Polymers as Hydroxide Exchange Membranes. *ChemSusChem* **3**, 555-558 (2010).
18. Gu, S. *et al.* Cover Picture: A Soluble and Highly Conductive Ionomer for High-Performance Hydroxide Exchange Membrane Fuel Cells (Angew. Chem. Int. Ed. 35/2009). *Angewandte Chemie International Edition* **48**, 6363-6363 (2009).
19. Gu, S., Cai, R. & Yan, Y. Self-crosslinking for dimensionally stable and solvent-resistant quaternary phosphonium based hydroxide exchange membranes. *Chem. Commun.* **47**, 2856-2858 (2011).
20. Stoica, D., Ogier, L., Akrou, L., Alloin, F. & Fauvarque, J. Anionic membrane based on polyepichlorhydrin matrix for alkaline fuel cell: Synthesis, physical and electrochemical properties. *Electrochim. Acta* **53**, 1596 (2007).

Appendix

RAW DATA FOR WATER UPTAKE AND SWELLING RATIO

Table A6: Raw Data for Water Uptake and Swelling Ratio Experiments

Mole Ratio	Rep	l_{wet1} (cm)	l_{wet2} (cm)	l_{wet} (cm)	l_{dry1} (cm)	l_{dry2} (cm)	l_{dry} (cm)	W_{wet} (g)	W_{dry} (g)
1:1.5	1	2.3	1.5	1.857	2.1	1.4	1.714	0.1272	0.1014
	2	2.4	1.5	1.897	2.2	1.4	1.754	0.1222	0.0988
1:2	1	2.8	1.6	2.116	2.6	1.45	1.942	0.1539	0.1275
	2	2.8	1.6	2.116	2.7	1.4	1.944	0.1587	0.1325